Photochemistry

Special Collection

Effect of the PHY Domain on the Photoisomerization Step of the Forward $P_r \rightarrow P_{fr}$ Conversion of a Knotless Phytochrome

Tobias Fischer,[a] Qianzhao Xu,[b] Kai-Hong Zhao,[c] Wolfgang Gärtner,[b] Chavdar Slavov,*[a] and Josef Wachtveitl*[a]

Abstract: Phytochrome photoreceptors operate via photoisomerization of a bound bilin chromophore. Their typical architecture consists of GAF, PAS and PHY domains. Knotless phytochromes lack the PAS domain, while retaining photoconversion abilities, with some being able to photoconvert with just the GAF domain. Therefore, we investigated the ultrafast photoisomerization of the P_r state of a knotless phytochrome to reveal the effect of the PHY domain and its "tongue" region on the transduction of the light signal. We show that the PHY domain does not affect the initial conformational dynamics of the chromophore. However, it significantly accelerates the consecutively induced reorganizational dynamics of the protein, necessary for the progression of the photoisomerization. Consequently, the PHY domain keeps the bilin and its binding pocket in a more reactive conformation, which decreases the extent of protein reorganization required for the chromophore isomerization. Thereby, less energy is lost along nonproductive reaction pathways, resulting in increased efficiency.

Introduction

Phytochromes are bilin-binding photoreceptors that regulate various biologically relevant processes (e.g., photosynthesis, morphogenesis, phototaxis, and photoprotection).[1,2] They function via a light-induced transformation between a thermostable parental state and a photoproduct state. The transformation is triggered by a $Z \rightleftharpoons E$ photoisomerization of the $C_{15} = C_{16}$ double bond and a subsequent rotation of the D-ring of the embedded bilin chromophore (Scheme 1).

Phytochromes consist of chromophore-binding GAF domains, PAS and PHY domains (Figure 1).[1,2] The PHY domain

forms an antiparallel β-sheet ("tongue") which interacts with the chromophore embedded in the GAF domain, and the PAS and the GAF domains form a figure-eight knot.[1,2] A complete PAS-GAF-PHY array is required for photoconversion in canonical phytochromes (e.g., PhyA, Cph1, Agp1),[3–5] while knotless phytochromes (e.g., Cph2)[6,7] lack the PAS domain.[1,2]

Interestingly, single GAF domains of cyanobacteriochromes (CBCRs)[9] and some knotless phytochromes[8,10] preserve their photoconversion capability, which makes them attractive for biotechnological applications.[11,12] The parental and the photoproduct states of canonical and knotless phytochromes are red-light (P_r) and far-red-light (P_{fr}) absorbing, respectively.[5] The photoisomerization reaction and the primary photoproduct (Lumi-R) formation in the forward ($P_r \rightarrow P_{fr}$) photoconversion of these phytochromes proceeds with a lifetime of tens[13–20] to hundreds[21–25] of picoseconds. Photoisomerization in other mo-

[a] T. Fischer, Dr. C. Slavov, Prof. J. Wachtveitl
Institute of Physical and Theoretical Chemistry
Goethe University Frankfurt am Main
Max-von-Laue Straße 7, 60438 Frankfurt (Germany)
E-mail: chslavov@theochem.uni-frankfurt.de
wveitl@theochem.uni-frankfurt.de

[b] Q. Xu, Prof. W. Gärtner
Institute of Analytical Chemistry
University of Leipzig
Linnéstr. 3, 04103 Leipzig (Germany)

[c] Prof. K.-H. Zhao
Key State Laboratory of Agriculture Microbiology
Huazhong Agriculture University Wuhan
Shizishan Street, Hongshan District, Wuhan 430070 (P. R. China)

Supporting information and the ORCID identification number(s) for the author(s) of this article can be found under:
https://doi.org/10.1002/chem.202003138.
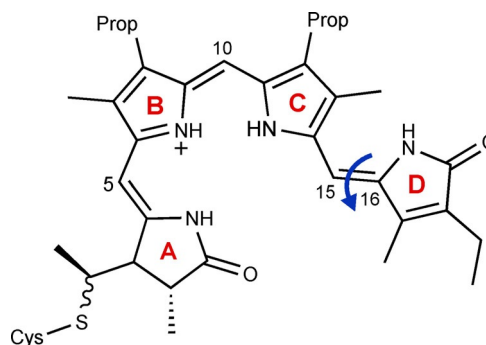
Scheme 1. Chemical structure of the phycocyanobilin (PCB) chromophore. The arrow indicates the photoisomerization of the $C_{15} = C_{16}$ double bond and the counterclockwise rotation of ring D.[8]

Chemistry–A European Journal

Full Paper
doi.org/10.1002/chem.202003138

Chemistry
Europe
European Chemical
Societies Publishing

lecular systems (e.g., azobenzenes[26,27] and rhodopsins[28–30]) is typically ultrafast, which raises the question about the origin of the remarkably slow photoisomerization rates in phytochromes. Recently, we could show that the excited state decay kinetics in a single GAF domain (g1) derived from a knotless phytochrome (All2699g1g2 from *Nostoc* sp. PCC7120) is strongly distributed, and we assigned this behavior to conformational changes in the bilin-binding pocket that control the photoisomerization of the chromophore.[8] Here, we report on the forward ($P_r{\rightarrow}P_{fr}$) photoisomerization dynamics of the complete knotless phytochrome All2699g1g2 (structurally similar to Cph2).[31,32] The homology model of All2699g1g2[32] (Figure 1) shows that the "tongue" region of the g2 domain interacts with the chromophore bound to g1, just like the PHY domains of canonical phytochromes. Therefore, the g1g2 construct provides a unique opportunity to directly evaluate the role of the "tongue" and thereby of the protein matrix in the photoisomerization of phytochromes. Furthermore, our results give insight into the photochemistry of knotless phytochromes, as their ultrafast dynamics has not been studied previously.
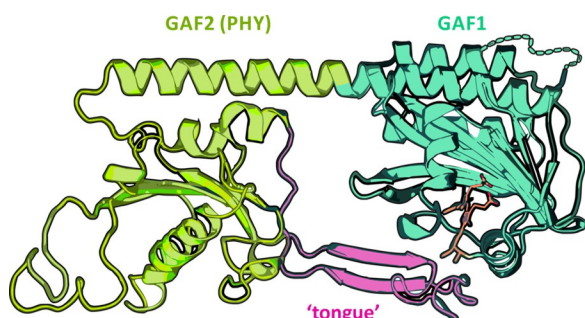

Figure 1. Schematic representation of the structural homology model of the P_r state of the All2699g1g2 construct.[32] The structure of the GAF1 domain is based on the crystal structure of the sole GAF1 module (PDB ID 6OZA), while the GAF2 domain was modelled based on the crystal structure of the structurally similar Cph2[32] (PDB ID 4BWI). The PCB chromophore (orange) embedded in the GAF1 domain (green) is in close interaction with a tongue-like protrusion (pink) from the GAF2 domain (yellow), which also shields the PCB from the solvent.

Results and Discussion

Photochromism of All2699 g1 g2

The P_r form of g1g2 has an absorption maximum at 637 nm, which is similar to that in g1,[8,33] while the P_{fr} form is significantly red shifted (by 73 nm) to 710 nm (689 nm in g1;[8,33] Figure 2A). Thus, the observed spectral shift of P_{fr} appears to be induced by interactions of the PCB chromophore with the "tongue" region of the g2 domain in g1g2.[32,34] Interestingly, we find that the quantum yield (QY) of the $P_r{\rightarrow}P_{fr}$ transition is increased from ~8% to ~13% (a similar QY is observed in the related Cph2[35]). Hence, it follows that while the presence of the g2 domain does not directly affect the spectral properties of the P_r form it does affect its photochemistry.

The circular dichroism (CD) spectra of both proteins (g1g2 vs. g1) have similar shape and undergo a sign inversion of the
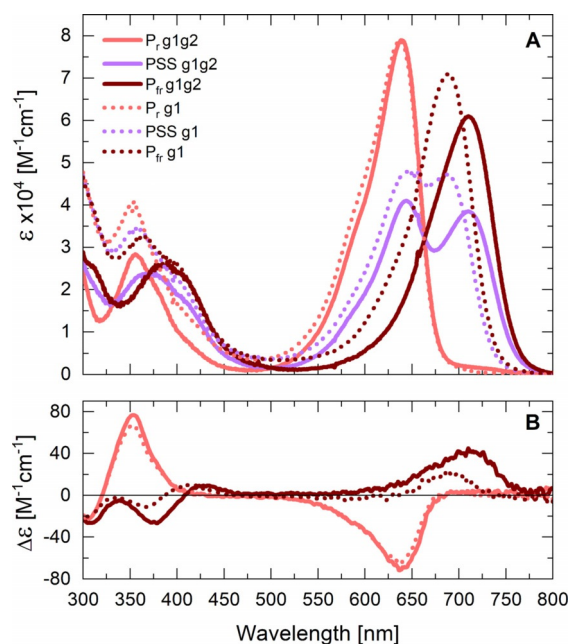

Figure 2. A) Stationary absorption spectra of the P_r and P_{fr} forms of g1g2 (solid lines) and g1[8] (dotted lines). The pure P_{fr} spectrum was obtained by conservative subtraction of 38% of the pure P_r spectrum from the PSS spectrum, followed by multiplication with a factor of 1.61 to yield the spectrum for the fully converted system. The extinction coefficient of P_r is ~79000 M^{-1} cm^{-1} (similar to g1[33]), while the extinction coefficient of P_{fr} is ~61000 M^{-1} cm^{-1}. B) CD spectra of the P_r and P_{fr} states of g1g2 (solid lines) and g1[8] (dotted lines). The pure P_{fr} CD spectrum was derived from the PSS CD as described in A).

Q-band CD signal upon $P_r{\leftrightarrow}P_{fr}$ switching (Figure 2B).[8,33] The Q-band CD signals exhibit opposite signs for the different states, negative for P_r and positive for P_{fr}. The P_{fr} signal of g1g2 is further red shifted and shows an increased extinction coefficient.

The signs of these signals indicate the orientation of the peripheral rings A and D with respect to the co-plane of rings B and C.[8,36] This overall orientation appears unaffected by the presence of the "tongue", which is in line with the slight changes in the dihedral angle of rings A and D observed by NMR.[32] In comparison, other phytochromes like Cph1[37] and Cph2[35] exhibit a similar sign change of the Q-band, while most CBCRs and bacteriophytochromes show no sign change upon switching.[36,38–40]

Ultrafast dynamics of $P_r{}^*$ and formation of Lumi-R

The role of the protein environment on the ultrafast photoisomerization dynamics of the PCB chromophore was investigated by femtosecond transient absorption (TA) measurements on g1g2 as compared with the single-domain g1.[8] The TA data of g1g2 show three main features (Figure 3A): i) a broad positive signal below 575 nm which can be assigned to excited state absorption (ESA), ii) a negative signal above 575 nm due to ground state bleach (GSB) and stimulated emission (SE), and iii) a positive photoproduct absorption (PA) appearing at later times at 670 nm associated with the formation of the primary
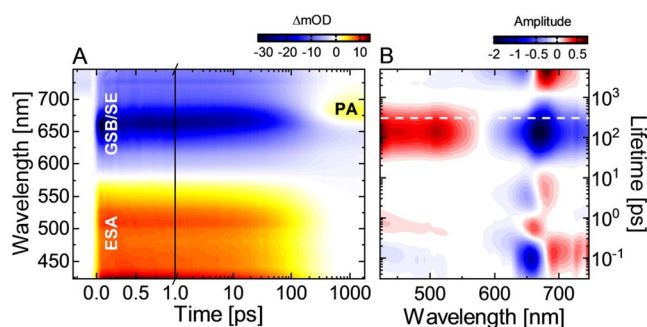
Chemistry–A European Journal

Full Paper
doi.org/10.1002/chem.202003138

Chemistry Europe
European Chemical
Societies Publishing

Figure 3. A) TA data from the forward, $P_r \rightarrow P_{fr}$, dynamics of g1g2 after 635 nm excitation. B) Corresponding lifetime density map (LDM) obtained from the lifetime distribution analysis of the TA data. The reading of the LDMs is as for a decay-associated spectrum from global lifetime analysis: i) positive (red) amplitudes account for decay of excited state and product absorption (ESA, PA) or rise of ground state bleach and stimulated emission (GSB and SE); ii) negative (blue) amplitudes account for rise of absorption (ESA, PA) or decay of GSB and SE. The white dashed line indicates the center of the lifetime distribution of the P_r^* decay of g1.[8]

photoproduct (Lumi-R). The rise of the Lumi-R signal coincides with the decay of the ESA, GSB and SE on the timescale of 100 to 400 ps.

The lifetime distribution analysis of the experimental data (see Supporting Information and Ref. [41] for methodology) gives further insight into the early ES dynamics of P_r (Figure 3B). The positive- (>690 nm) and the negative-amplitude (<690 nm) distributions with a lifetime of 100 fs can be assigned to a red shift of the SE and therefore to the departure of the ES wavepacket from the Franck-Condon (FC) region. The lifetime distributions between 1 ps and 10 ps are located at the overlap of the steep edges of the GSB and SE, making this region very sensitive to slight spectral changes.

Because there is no substantial decay of the ES on this timescale, we assign these distributions to dynamics on the ES potential energy surface. Based on the spectral position of the ESA, GSB and SE signals, the broad lifetime distributions (stretching from 30 ps to 1 ns) with positive (420–575 nm) and negative (600–740 nm) amplitudes can be attributed to the simultaneous decay of these signals, and thus to the decay of P_r^*.

Compared with the positive-amplitude distribution representing the decay of the ESA signal, the negative-amplitude distribution, especially at 675 nm, appears stretched in lifetime. This can be explained by an overlaid additional negative-amplitude distribution describing the rise of the primary photoproduct Lumi-R commencing with the ES decay. On the scale longer than 1 ns, the negative and positive-amplitude lifetime distributions correspond to the non-decaying GSB and Lumi-R signals.

Distributed character of the P_r^* photoisomerization kinetics

Previously, we showed that the P_r^* decay kinetics in the single-domain g1 is described by broad and structureless lifetime distributions (see Figure S2B and discussion in[8]) and can be modelled well using a stretched exponential function,[42,43] thereby

avoiding introduction of unnecessary kinetic components. The lifetime distributions describing the P_r^* decay of g1g2 (from 30 ps to 1 ns in Figure 3B) are similarly broad and structureless, thus we followed our previous approach and analyzed the TA data using a four-state model in which one of the states is modelled by a stretched exponent (Figure 4). This model yields an excellent fit of the data without additional kinetic components (compare the case of the five-state model (Figure S5)). Stretched exponentials are used to model distributed kinetics occurring in constrained environments[44–46] and here underline the importance of the protein in the isomerization kinetics of the PCB chromophore.

The evolutionary associated difference spectra (EADS) of the first three states (Figure 4B) clearly show that at early times no significant change in the amplitude of the ESA occurs, reaffirming the conclusion that the sub-20 ps dynamics of P_r^* is not associated with ES decay. Therefore, similarly to the single GAF domains All2699g1[8] and Slr1393g3,[47] the EADS of S2 and S3 of g1g2 show only a minor spectral shift in the GSB and SE overlap area, indicating that the ~3 ps component (Figure 4) is due to ES dynamics of the chromophore. The P_r^* relaxation and the associated PCB photoisomerization occur on the 100 ps timescale from state S3 after overcoming a barrier on the ES potential energy surface.[8] This state is modeled as a stretched exponent, showing that the P_r^* decay of g1g2 follows a distributed type kinetics.

Recently, it was reported that in g1 and in g1g2 there exists a broad distribution of ground state subconformations that rapidly interconvert in solution.[32,48] These subconformations could partially contribute to the observed distributed character of the P_r^* decay kinetics. However, their rapid interconversion denotes that they are separated by low energetic barriers, and thus cannot explain the large excited state barrier that determines the relatively slow P_r^* decay kinetics (100 ps timescale).[8] Such a barrier can be overcome only via dynamic reorganization of the system, which in turn provides the dominant contribution to the distributed kinetics of P_r^* decay. Therefore, our
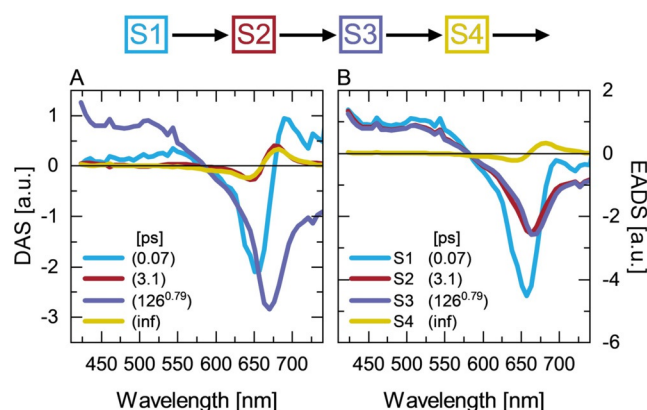

Figure 4. Analysis of the experimental data from the $P_r \rightarrow P_{fr}$ dynamics of g1g2 after 635 nm excitation using a sequential kinetic scheme. The kinetic model fitting results in the so-called evolution-associated difference spectra (EADS) and decay associated spectra (DAS): A) DAS and B) EADS from fitting a sequential scheme with four states, with the third state (S3) being modeled with a stretched exponent with $\beta = 0.79$.

Chemistry–A European Journal | Full Paper
doi.org/10.1002/chem.202003138

**Chemistry
Europe**
European Chemical
Societies Publishing

results point to a more dynamic picture of the kinetics in knot-less phytochromes. In contrast, distinct ES decay components, including such on the sub-50 ps timescale, have been reported for other phytochromes (e.g., Cph1, PhyA) and CBCRs, and were discussed in the framework of static ground state heterogeneity of the P_r form.[15,18,20,38,49,50]

Comparison of the ultrafast dynamics of g1g2 and g1: the effect of the g2 (PHY) domain

The comparison of the ultrafast dynamics of the g1g2 construct with the dynamics of the sole GAF domain g1[8] provides a direct assessment of the effect of the g2 (PHY) domain. Strikingly, the early dynamics of both proteins are identical and even the coherent oscillations observed in the SE region up to ∼2 ps (Figure 5 B) match in frequency and phase.

The similarity in the g1g2 and g1 early kinetics is in agreement with the lack of an immediate effect of the PHY domain on the steady state properties of the P_r form (Figure 2), and thus further supports the conclusion that the primary dynamics are indeed due to conformational changes in the PCB chromophore. Only at later times, the P_r^* kinetics of g1g2 deviates from that of g1. Figure 5 clearly shows that in the g1g2 construct the ES decay and the formation of the primary photoproduct Lumi-R are accelerated relative to g1. This effect is also illustrated by the corresponding LDMs (Figure S2). Considering the time range up to 10 ps, the lifetime distribution structure remains the same for both proteins, while the later lifetime distributions (from 30 ps to 1 ns) describing the ES decay are shifted to shorter lifetimes in the case of g1g2 (for comparison, the center lifetime of the corresponding g1 distribution is indicated by a white dashed line in the LDM of g1g2, Figure 3 B). Therefore, the direct comparison of the P_r^* kinetics

of g1g2 and g1 reveals the impact of the g2 (PHY) domain and categorically demonstrates the critical role of the protein environment on the photoisomerization step of the PCB chromophore.

Mechanistic model

Based on the analysis presented above, we propose the following molecular picture for the photoisomerization dynamics of g1g2 (Figure 6). After excitation, the PCB chromophore leaves the FC region (∼100 fs) and undergoes ES conformational dynamics on the early ps timescale (<20 ps). This dynamics acts as a trigger for larger scale motions in the protein environment, which alleviates restrictions hindering further evolution on the ES (illustrated by the barrier on the ES potential energy surface). Interestingly, similar conclusions were derived in recent studies on related bacteriophytochromes[51,52] and a cyanobacteriochrome.[53] As the protein reorganizes, the barrier on the ES decreases which allows P_r^* relaxation to proceed. This model explains the distributed character of the P_r^* decay kinetics as it is imposed by the conformational dynamics of the protein. Eventually, P_r^* decays (∼130 ps) yielding the primary photoproduct Lumi-R.

Previously, we demonstrated that the ring D rotation of the PCB chromophore in g1 is hindered by a nearby Tyr residue (Tyr142).[8] In the g1g2 (GAF-PHY) construct, the interaction of
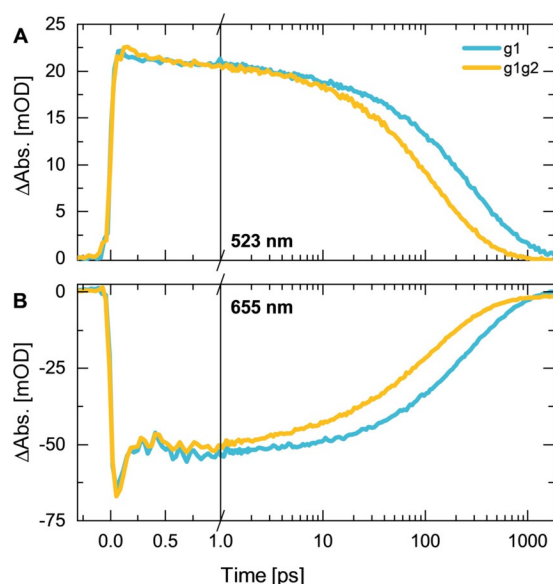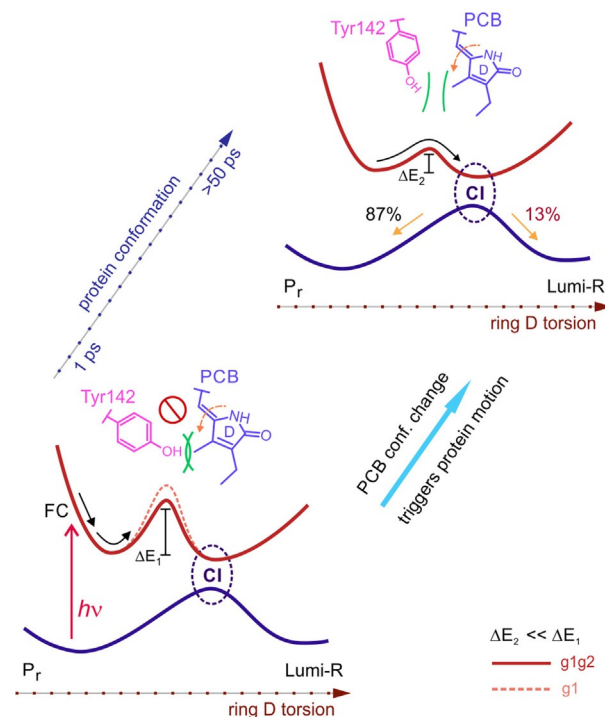

Figure 5. Comparison of the transient absorption decays of g1g2 (orange) and g1[8] (cyan) at selected wavelengths within A) the ESA (523 nm), and B) the GSB/SE (655 nm) spectral regions. The transient decays were measured after 635 nm excitation of the P_r form.

Figure 6. Main reaction coordinates determining the photoconversion kinetics in the P_r form of g1 and g1g2. For the larger construct, the interaction of the "tongue" region with the PCB chromophore results in a lower barrier (red, solid vs. orange, dashed lines). The early (<10 ps) dynamics of the PCB chromophore triggers reorganizations in the protein binding pocket, which lower the energetic barrier at later timescales (ΔE₁ vs. ΔE₂) and unlock the photoisomerization.

Chemistry–A European Journal

Full Paper
doi.org/10.1002/chem.202003138

Chemistry Europe
European Chemical
Societies Publishing

the "tongue" region of the PHY domain with the chromophore-binding pocket in the GAF domain limits the conformational space of rings A and D of the PCB and drives the Tyr142 residue away from the chromophore as compared with g1.[32] Therefore, it appears as if the "tongue" region keeps the chromophore and the binding pocket in a more reactive conformation. This decreases the extent of protein conformation reorganization required for facilitating the isomerization of the PCB chromophore and results in an accelerated P_r^* decay kinetics (Figure 5) and a more efficient $P_r \rightarrow P_{fr}$ photoconversion (less energy being lost on nonproductive degrees of freedom).

Conclusions

Our work provides direct evidence for the essential role of the protein environment in the control of the photoisomerization kinetics of the PCB chromophore and outlines a detailed mechanistic picture of the P_r^* photoisomerization dynamics in knotless phytochromes. From an evolutionary perspective, the PHY domain "tongue" represents a development in phytochromes that tunes the photoreception efficiency. This is a key design principle for the development of optimized photoreceptors for biotechnological applications.

Acknowledgements

Conflict of interest

The authors declare no conflict of interest.

[1] K. Anders, L. O. Essen, *Curr. Opin. Struct. Biol.* **2015**, *35*, 7–16.
[2] N. C. Rockwell, J. C. Lagarias, *Curr. Opin. Plant Biol.* **2017**, *37*, 87–93.
[3] N. C. Rockwell, J. C. Lagarias, *Plant Cell* **2006**, *18*, 4–14.
[4] A. Möglich, X. Yang, R. A. Ayers, K. Moffat, *Annu. Rev. Plant Biol.* **2010**, *61*, 21–47.
[5] N. C. Rockwell, Y.-S. Su, J. C. Lagarias, *Annu. Rev. Plant Biol.* **2006**, *57*, 837–858.
[6] C. M. Park, J. I. Kim, S. S. Yang, J. G. Kang, J. H. Kang, J. Y. Shim, Y. H. Chung, Y. M. Park, P. S. Song, *Biochemistry* **2000**, *39*, 10840–10847.
[7] B. L. Montgomery, J. C. Lagarias, *Trends Plant Sci.* **2002**, *7*, 357–366.
[8] C. Slavov, T. Fischer, A. Barnoy, H. Shin, A. G. Rao, C. Wiebeler, Y. Zeng, Y. Sun, Q. Xu, A. Gutt, K. Zhao, W. Gärtner, X. Yang, I. Schapiro, J. Wachtveitl, *Proc. Natl. Acad. Sci. USA* **2020**, *117*, 16356–16362.
[9] M. Ikeuchi, T. Ishizuka, *Photochem. Photobiol. Sci.* **2008**, *7*, 1159.
[10] A. T. Ulijasz, G. Cornilescu, D. Von Stetten, S. Kaminski, M. A. Mroginski, J. Zhang, D. Bhaya, P. Hildebrandt, R. D. Vierstra, *J. Biol. Chem.* **2008**, *283*, 21251–21256.
[11] C. Gasser, S. Taiber, C. M. Yeh, C. H. Wittig, P. Hegemannd, S. Ryu, F. Wunder, A. Möglich, *Proc. Natl. Acad. Sci. USA* **2014**, *111*, 8803–8808.
[12] O. S. Oliinyk, A. A. Shemetov, S. Pletnev, D. M. Shcherbakova, V. V. Verkhusha, *Nat. Commun.* **2019**, *10*, 1–13.
[13] M. Bischoff, G. Hermann, S. Rentsch, D. Strehlow, *Biochemistry* **2001**, *40*, 181–186.
[14] C. Schumann, R. Groß, N. Michael, T. Lamparter, R. Diller, *ChemPhysChem* **2007**, *8*, 1657–1663.
[15] M. G. Müller, I. Lindner, I. Martin, W. Gärtner, A. R. Holzwarth, *Biophys. J.* **2008**, *94*, 4370–4382.
[16] J. Dasgupta, R. R. Frontiera, K. C. Taylor, J. C. Lagarias, R. A. Mathies, *Proc. Natl. Acad. Sci. USA* **2009**, *106*, 1784–1789.
[17] Y. Yang, M. Linke, T. von Haimberger, J. Hahn, R. Matute, L. González, P. Schmieder, K. Heyne, *J. Am. Chem. Soc.* **2012**, *134*, 1408–1411.
[18] Y. Yang, M. Linke, T. von Haimberger, R. Matute, L. González, P. Schmieder, K. Heyne, *Struct. Dyn.* **2014**, *1*, 014701.
[19] K. Heyne, J. Herbst, D. Stehlik, B. Esteban, T. Lamparter, J. Hughes, R. Diller, *Biophys. J.* **2002**, *82*, 1004–1016.
[20] P. W. Kim, N. C. Rockwell, S. S. Martin, J. C. Lagarias, D. S. Larsen, *Biochemistry* **2014**, *53*, 2818–2826.
[21] K. C. Toh, E. A. Stojković, I. H. M. M. Van Stokkum, K. Moffat, J. T. M. M. Kennis, *Proc. Natl. Acad. Sci. USA* **2010**, *107*, 9170–9175.
[22] H. Lehtivuori, I. Rissanen, H. Takala, J. Bamford, N. V. Tkachenko, J. A. Ihalainen, *J. Phys. Chem. B* **2013**, *117*, 11049–11057.
[23] T. Mathes, J. Ravensbergen, M. Kloz, T. Gleichmann, K. D. Gallagher, N. C. Woitowich, R. St. Peter, S. E. Kovaleva, E. A. Stojković, J. T. M. M. Kennis, *J. Phys. Chem. Lett.* **2015**, *6*, 239–243.
[24] P. Singer, S. Wörner, T. Lamparter, R. Diller, *ChemPhysChem* **2016**, *17*, 1288–1297.
[25] C. Wang, M. L. Flanagan, R. D. McGillicuddy, H. Zheng, A. R. Ginzburg, X. Yang, K. Moffat, G. S. Engel, *Biophys. J.* **2016**, *111*, 2125–2134.
[26] T. Nägele, R. Hoche, W. Zinth, J. Wachtveitl, *Chem. Phys. Lett.* **1997**, *272*, 489–495.
[27] A. Nenov, R. Borrego-Varillas, A. Oriana, L. Ganzer, F. Segatta, I. Conti, J. Segarra-Marti, J. Omachi, M. Dapor, S. Taioli, C. Manzoni, S. Mukamel, G. Cerullo, M. Garavelli, *J. Phys. Chem. Lett.* **2018**, *9*, 1534–1541.
[28] R. Schoenlein, L. Peteanu, R. Mathies, C. Shank, *Science* **1991**, *254*, 412–415.
[29] D. Polli, P. Altoè, O. Weingart, K. M. Spillane, C. Manzoni, D. Brida, G. Tomasello, G. Orlandi, P. Kukura, R. A. Mathies, M. Garavelli, G. Cerullo, *Nature* **2010**, *467*, 440–443.
[30] C. Bamann, E. Bamberg, J. Wachtveitl, C. Glaubitz, *Biochim. Biophys. Acta Bioenerg.* **2014**, *1837*, 614–625.
[31] K. Anders, G. Daminelli-Widany, M. A. Mroginski, D. Von Stetten, L. O. Essen, *J. Biol. Chem.* **2013**, *288*, 35714–35725.
[32] Q.-Z. Xu, P. Bielytskyi, J. Otis, C. Lang, J. Hughes, K.-H. Zhao, A. Losi, W. Gärtner, C. Song, *Int. J. Mol. Sci.* **2019**, *20*, 3656.
[33] Y. Chen, J. Zhang, J. Luo, J. M. Tu, X. L. Zeng, J. Xie, M. Zhou, J. Q. Zhao, H. Scheer, K. H. Zhao, *FEBS J.* **2012**, *279*, 40–54.
[34] Q.-Z. Xu, L. Goett-Zink, W. Gärtner, K.-H. Zhao, T. Kottke, *Biochemistry* **2020**, *59*, 2047–2054.
[35] K. Anders, D. Von Stetten, J. Mailliet, S. Kiontke, V. A. Sineshchekov, P. Hildebrandt, J. Hughes, L. O. Essen, *Photochem. Photobiol.* **2011**, *87*, 160–173.
[36] N. C. Rockwell, L. Shang, S. S. Martin, J. C. Lagarias, *Proc. Natl. Acad. Sci. USA* **2009**, *106*, 6123–6127.
[37] B. Borucki, H. Otto, G. Rottwinkel, J. Hughes, M. P. Heyn, T. Lamparter, *Biochemistry* **2003**, *42*, 13684–13697.
[38] P. W. Kim, L. H. Freer, N. C. Rockwell, S. S. Martin, J. C. Lagarias, D. S. Larsen, *Biochemistry* **2012**, *51*, 608–618.
[39] N. C. Rockwell, S. L. Njuguna, L. Roberts, E. Castillo, V. L. Parson, S. Dwojak, J. C. Lagarias, S. C. Spiller, *Biochemistry* **2008**, *47*, 7304–7316.
[40] Y. Hirose, N. C. Rockwell, K. Nishiyama, R. Narikawa, Y. Ukaji, K. Inomata, J. C. Lagarias, M. Ikeuchi, *Proc. Natl. Acad. Sci. USA* **2013**, *110*, 4974–4979.
[41] C. Slavov, H. Hartmann, J. Wachtveitl, *Anal. Chem.* **2015**, *87*, 2328–2336.
[42] R. Kohlrausch, *Ann. Phys. Chem.* **1854**, *167*, 179–214.
[43] G. Williams, D. C. Watts, *Trans. Faraday Soc.* **1970**, *66*, 80–85.

[44] H. Frauenfelder, S. G. Sligar, P. G. Wolynes, *Science* **1991**, *254*, 1598–1603.

[45] H. Yang, G. Luo, P. Karnchanaphanurach, T.-M. M. Louie, I. Rech, S. Cova, L. Xun, X. S. Xie, *Science* **2003**, *302*, 262–266.

[46] O. Flomenbom, K. Velonia, D. Loos, S. Masuo, M. Cotlet, Y. Engelborghs, J. Hofkens, A. E. Rowan, R. J. M. Nolte, M. Der Van Auweraer, F. C. De Schryver, J. Klafter, *Proc. Natl. Acad. Sci. USA* **2005**, *102*, 2368–2372.

[47] C. Slavov, X. Xu, K. H. Zhao, W. Gärtner, J. Wachtveitl, *Biochim. Biophys. Acta Bioenerg.* **2015**, *1847*, 1335–1344.

[48] Y. Kim, Q.-Z. Xu, K.-H. Zhao, W. Gärtner, J. Matysik, C. Song, *J. Phys. Chem. B* **2020**, *124*, 7115–7127.

[49] P. W. Kim, N. C. Rockwell, L. H. Freer, C.-W. W. Chang, S. S. Martin, J. C. Lagarias, D. S. Larsen, *J. Phys. Chem. Lett.* **2013**, *4*, 2605–2609.

[50] J. S. Kirpich, L. T. Mix, S. S. Martin, N. C. Rockwell, J. C. Lagarias, D. S. Larsen, *J. Phys. Chem. Lett.* **2018**, *9*, 3454–3462.

[51] E. Claesson, W. Y. Wahlgren, H. Takala, S. Pandey, L. Castillon, V. Kuznetsova, L. Henry, M. Panman, M. Carrillo, J. Kübel, R. Nanekar, L. Isaksson, A. Nimmrich, A. Cellini, D. Morozov, M. Maj, M. Kurttila, R. Bosman, E. Nango, R. Tanaka, T. Tanaka, L. Fangjia, S. Iwata, S. Owada, K. Moffat, G. Groenhof, E. A. Stojković, J. A. Ihalainen, M. Schmidt, S. Westenhoff, *eLife* **2020**, *9*, 1–18.

[52] D. Wang, Y. Qin, M. Zhang, X. Li, L. Wang, X. Yang, D. Zhong, *J. Phys. Chem. Lett.* **2020**, *11*, 5913–5919.

[53] D. Wang, X. Li, L. Wang, X. Yang, D. Zhong, *J. Phys. Chem. Lett.* **2020**, *11*, 8819–8824.